



Citation for published version:

Carley, MJ & Martin, PA 2012, 'Jet noise: sound generation by disc and cylinder sources', Proceedings of the Royal Society of London Series A - Mathematical Physical and Engineering Sciences, vol. 468, no. 2148, pp. 3947-3964. <https://doi.org/10.1098/rspa.2012.0362>

DOI:

[10.1098/rspa.2012.0362](https://doi.org/10.1098/rspa.2012.0362)

Publication date:

2012

Document Version

Peer reviewed version

[Link to publication](#)

University of Bath

General rights

Copyright and moral rights for the publications made accessible in the public portal are retained by the authors and/or other copyright owners and it is a condition of accessing publications that users recognise and abide by the legal requirements associated with these rights.

Take down policy

If you believe that this document breaches copyright please contact us providing details, and we will remove access to the work immediately and investigate your claim.

Jet noise: sound generation by disc and cylinder sources

M. J. Carley¹ and P. A. Martin²

¹*Department of Mechanical Engineering, University of Bath, Bath BA2 7AY, UK*

²*Department of Applied Mathematics and Statistics, Colorado School of Mines, Golden, CO 80401-1887, USA*

An exact analysis of the field radiated by tonal and random non-axisymmetric sources distributed over a disc or cylinder is presented. The analysis is exact, without recourse to near- or far-field approximations, and leads to a direct relationship between source frequency and the nature of the radiated field. The implications of the analysis for a number of applications are discussed, finding in particular that: source identification is inherently ill-conditioned as a result of a ‘filtering’ effect which removes information from the radiation field; low-frequency sources generate fields which are indistinguishable from each other; jet noise fields are inherently simpler than the flow which gives rise to them, a finding which has previously been noted for experimental data.

1. Introduction

A common problem in the prediction of acoustic, and other, radiation is that of calculating the field produced by a source distributed over a disc or a cylinder, such as loudspeakers, rotors, duct terminations, and turbulent jets. There is an extensive literature on these fields, in acoustics, as well as in allied fields such as electromagnetism and optics. This paper presents an exact analysis of such fields, which can be used to draw conclusions about the nature of the field and about a number of problems which arise from it. The analysis was motivated by problems in acoustics, and will be described in these terms, but it should apply to any system governed by a retarded potential.

In the first part of the analysis, a disc source whose strength varies periodically in azimuth is considered, corresponding to the problem of a tonal sound field. This is a generalization of the familiar problem of radiation from an axisymmetric circular baffled piston (Pierce, 1989) which has led to the division of the field into a near and far, or radiation, field. The nature of these regions for a non-axisymmetric source has been examined previously Chapman (1993), with application to high speed rotor noise. It was found that an exponentially

small amount of energy ‘tunnels’ across the boundary between the near and far fields, with the form of the field being set by the relationship of source radius and frequency.

This analysis has been extended to consider the ‘information content’ of the field (Carley, 2011), showing that the radiated field has a limited number of degrees of freedom, the number being fixed by the source frequency. This is especially relevant to the inverse problem, where acoustic field measurements are used to attempt to infer the nature of the source, such as for aircraft engines (Gérard *et al.*, 2007; Holste & Neise, 1997; Lewy, 2008; Castres & Joseph, 2007*a,b*, for example). It has been recognized that the inverse problem is poorly conditioned, requiring special numerical methods for its treatment. Our analysis will demonstrate that this ill conditioning is an unavoidable result of the nature of the source and that there is a limit on the information available for source identification. It is well-known that due to the arbitrary nature of source terms (Ffowcs Williams, 1984), and the filtering effect of propagation, which removes source terms with subsonic phase velocity (Carley, 2010), there is no unambiguous relationship which characterizes a source using only field information.

Acoustic field measurements have also been used to try to characterize the noise source in turbulent jets, such as in the near- to far-field correlation technique (Laurendeau *et al.*, 2008), where it is assumed that the near field data ‘encode’ source information, so that they can be used to draw inferences about the relationship between the source and the radiated noise field. The nature of the jet noise field, and of its relationship to the acoustic source, has long been of interest, and a number of recent experimental and computational studies have produced unexpected results on the relationship between the source and field.

It has long been accepted that turbulent jets are inefficient acoustic radiators, but it is only recently that it has been possible to quantify the simplicity of the noise field, compared to the complexity of the turbulent velocity field of the jet proper. In these studies (Jordan *et al.*, 2007; Schlegel *et al.*, 2012), it has been found that in a Mach 0.9 jet, 90% of the acoustic field energy could be resolved using 24 orthogonal modes, while 350 were required to capture only 50% of the flow energy. A number of explanations have been given for this relative simplicity of the acoustic field such as source cancellation Michel (2007, 2009) and spatial filtering of the source Freund (2001).

Our analysis gives an exact formulation for the field radiated by tonal and by random sources, which gives a framework for the understanding of these questions, without requiring assumptions about the nature of the source. In particular, it explains the limits on the source information radiated into the field and allows us to explain many of the features which we have just described.

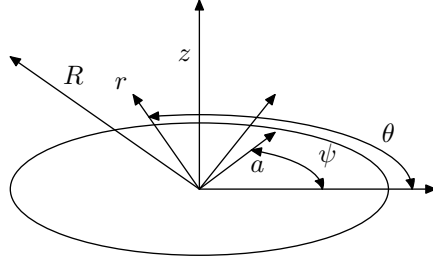


Figure 1. Coordinate system for disc radiation calculations

2. Disc source

The problem is initially formulated as that of calculating the acoustic field radiated by a monopole source distributed over a circular disc. The system for the analysis is shown in figure 1 with cylindrical coordinates (r, θ, z) for the observer and $(a, \psi, 0)$ for the source. All lengths are non-dimensionalized on disc radius. The field from one azimuthal mode of the acoustic source, specified as $s_n(a) \exp i[n\psi - \omega t]$, has the form $P_n(k, r, z) \exp i[n\theta - \omega t]$, with P_n given by the Rayleigh integral (Goldstein, 1974; Carley, 2009),

$$P_n(k, r, z) = \int_0^1 \int_{-\pi}^{\pi} \frac{e^{i(kR+n\psi)}}{4\pi R} s_n(a) a \, d\psi \, da, \quad (2.1)$$

where $R = \sqrt{r^2 + a^2 - 2ra \cos \psi + z^2}$ and k is non-dimensional wavenumber.

The analysis which follows gives an exact formulation for the field radiated by tonal and by random sources, similar to previous work, but with efficient series expansions for radiation calculations (§a), explicit integral and asymptotic formulae for the source terms (§b, and extension to arbitrary frequency and azimuthal mode number for random sources (§d).

(a) Tonal disc source

The analysis of the nature of the sound field from an arbitrary disc source is based on a transformation of the disc to an exactly equivalent line source, shown in figure 2, which shows the new coordinate system (s_2, θ_2, z) centred on a sideline of constant radius $r > 1$. Under this transformation (Carley, 2009), which gathers terms of constant phase to reduce the double integral to a set of

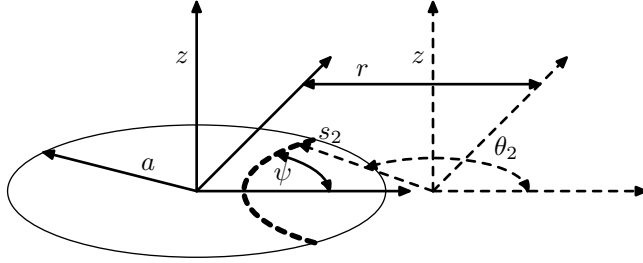


Figure 2. Transformation to equivalent line source

single integrals:

$$P_n(k, r, z) = \int_{r-1}^{r+1} \frac{e^{ik\sqrt{s_2^2+z^2}}}{\sqrt{s_2^2+z^2}} K_n(r, s_2) s_2 ds_2, \quad (2.2)$$

$$K_n(r, s_2) = \frac{1}{4\pi} \int_{\theta_2^{(0)}}^{2\pi-\theta_2^{(0)}} e^{in\psi} s_n(a) d\theta_2, \quad (2.3)$$

with $\theta_2^{(0)} = \cos^{-1} [(1 - r^2 - s_2^2)/(2rs_2)]$. Functions of the form of $K_n(r, s_2)$ have been analyzed in previous work (Carley, 2010) and can be written as

$$K_n(r, s_2) = \sum_{q=0}^{\infty} u_q^n(r) U_q(s)(1 - s^2)^{1/2}, \quad (2.4)$$

where $U_q(s)$ is a Chebyshev polynomial of the second kind, $s = s_2 - r$ and the coefficients $u_q^n(r)$ are functions of r but not of z . Inserting (2.4) into (2.2) gives

$$P_n(k, r, z) = \sum_{q=0}^{\infty} u_q^n(r) \mathcal{L}_q(k, r, z), \quad (2.5)$$

$$\mathcal{L}_q(k, r, z) = \int_{-1}^1 \frac{e^{ikR}}{R} U_q(s)(r + s)(1 - s^2)^{1/2} ds, \quad (2.6)$$

with $R = \sqrt{(r + s)^2 + z^2}$.

For $z = 0$, \mathcal{L}_q can be evaluated in closed form (Carley, 2010):

$$\mathcal{L}_q(k, r, 0) = i^q(q + 1)\pi e^{ikr} k^{-1} J_{q+1}(k). \quad (2.7)$$

For $z \neq 0$, there is no closed form solution for \mathcal{L}_q , but a series expansion is readily derived, based on a related integral containing the Chebyshev polynomial

of the first kind,

$$\Phi_q(k, r, z) = \int_{-1}^1 \frac{e^{ikR}}{R} T_q(s) (1 - s^2)^{-1/2} ds. \quad (2.8)$$

Put $r = \varrho \cos \varphi$ and $z = \varrho \sin \varphi$; note that φ is not the usual spherical polar coordinate. Then, using 8.533(1) from G&R (Gradshteyn & Ryzhik, 1980),

$$\Phi_q = ik \sum_{n=0}^{\infty} (2n+1) h_n^{(1)}(k\varrho) \mathcal{J}_{q,n}(k) P_n(\cos \varphi) [(-1)^q + (-1)^n], \quad (2.9)$$

where $h_n^{(1)}$ is a spherical Hankel function, P_n is a Legendre polynomial,

$$\mathcal{J}_{q,n} = \int_0^1 T_q(s) j_n(ks) (1 - s^2)^{-1/2} ds = \int_0^{\pi/2} j_n(k \cos \alpha) \cos q\alpha d\alpha \quad (2.10)$$

and j_n is a spherical Bessel function. Expanding j_n and integrating (G&R, 7.346) termwise gives an expansion for $\mathcal{J}_{q,n}(k)$ in powers of k .

Given a means of computing Φ_q , \mathcal{L}_q can be evaluated using standard relations for Chebyshev polynomials:

$$\mathcal{L}_q(k, r, z) = \frac{r}{2} (\Phi_q - \Phi_{q+2}) + \frac{1}{4} (\Phi_{q-1} - \Phi_{q+3}). \quad (2.11)$$

One motivation for working with the integral involving a Chebyshev polynomial of the first, rather than of the second, kind is that the form of the series (2.9) is simpler for Chebyshev polynomials of the first kind. Second, if \mathcal{L}_q is to be computed for various values of q , it is computationally simpler to compute Φ_q for the appropriate values of q and combine them as required in (2.11).

(b) Line source coefficients

Given the formulation of the radiation problem in terms of the equivalent line source, it remains to find the coefficients u_q^n in the expansion (2.4). These have been found previously (Carley, 2011) as the solution of an infinite system of equations, which, although correct, is poorly-conditioned and does not have an obvious explicit form. Here, we derive explicit, closed-form expressions for u_q^n as weighted integrals of the source term $s_n(a)$. This is done by equating two exact expressions for the field in the plane $z = 0$, using (2.7),

$$\int_0^1 \int_{-\pi}^{\pi} \frac{e^{i(kS+n\psi)}}{4\pi S} d\psi s_n(a) a da = \pi e^{ikr} \sum_{q=0}^{\infty} i^q (q+1) u_q^n \frac{J_{q+1}(k)}{k}, \quad (2.12)$$

with $S = \sqrt{r^2 + a^2 - 2ar \cos \psi}$. Note that, as $r > 1$, $|S - r| < 1$.

To derive an integral expression for the coefficients u_q^n , we begin by considering the corresponding expression for a ring source,

$$\frac{1}{4\pi} \int_{-\pi}^{\pi} \frac{1}{S} e^{ik(S-r)} e^{in\psi} d\psi = \sum_{q=0}^{\infty} i^q K_q^n(r, a) \frac{J_{q+1}(k)}{k}, \quad (2.13)$$

so that the line source coefficients for a disc source are given by

$$u_q^n(r) = \frac{1}{4(q+1)} \int_0^1 K_q^n(r, a) s_n(a) a da. \quad (2.14)$$

Let us split (2.13) into even and odd functions of k . We obtain

$$\frac{1}{2\pi} \int_0^{\pi} \frac{1}{S} \cos \{k(S-r)\} \cos n\psi d\psi = \sum_{q=0}^{\infty} (-1)^q K_{2q}^n(r, a) \frac{J_{2q+1}(k)}{k}, \quad (2.15)$$

$$\frac{1}{2\pi} \int_0^{\pi} \frac{1}{S} \sin \{k(S-r)\} \cos n\psi d\psi = \sum_{q=0}^{\infty} (-1)^q K_{2q+1}^n(r, a) \frac{J_{2q+2}(k)}{k}. \quad (2.16)$$

These show that K_q^n is real. Letting $k \rightarrow 0$ in (2.15) gives

$$K_0^n(r, a) = \frac{1}{\pi} \int_0^{\pi} \frac{1}{S} \cos n\psi d\psi. \quad (2.17)$$

Similarly, (2.16) gives

$$K_1^n(r, a) = \frac{4}{\pi} \int_0^{\pi} \frac{S-r}{S} \cos n\psi d\psi. \quad (2.18)$$

More generally, let us use the orthogonality integral (G&R, 6.538.2)

$$\int_0^{\infty} J_{2m+\nu}(k) J_{2n+\nu}(k) \frac{dk}{k} = \frac{\delta_{mn}}{4n+2\nu}, \quad \nu > 0.$$

Thus, multiplying (2.15) by $J_{2p+1}(k)$ and integrating over k gives

$$K_{2q}^n(r, a) = \frac{1}{\pi} (2q+1) (-1)^q \int_0^{\pi} \frac{\cos n\theta}{S} \int_0^{\infty} J_{2q+1}(k) \cos \{k(S-r)\} dk d\theta.$$

The inner integral is a Weber–Schafheitlin integral (G&R, 6.671.2): as $|S-r| < 1$, put $S-r = \sin \beta$ with $|\beta| < \frac{1}{2}\pi$, and then we obtain

$$K_{2q}^n(r, a) = \frac{1}{\pi} (2q+1) (-1)^q \int_0^{\pi} \frac{\cos n\psi}{S} \frac{\cos (2q+1)\beta}{\cos \beta} d\psi, \quad (2.19)$$

which reduces to (2.17) when $q = 0$.

For (2.16), we multiply by $J_{2p+2}(k)$ and integrate over k giving

$$K_{2q+1}^n(r, a) = \frac{(q+1)}{2\pi} (-1)^q \int_0^\pi \frac{\cos n\psi}{S} \int_0^\infty J_{2q+2}(k) \sin \{k(S-r)\} dk d\psi.$$

Evaluating the inner integral (G&R, 6.671.1) gives

$$K_{2q+1}^n(r, a) = \frac{(q+1)}{2\pi} (-1)^q \int_0^\pi \frac{\cos n\psi}{S} \frac{\sin (2q+2)\beta}{\cos \beta} d\psi, \quad (2.20)$$

with β defined as before. When $q=0$, this formula reduces to (2.18).

Expanding $\cos n\beta$ and $\sin n\beta$ in powers of $\sin \beta$ and thus in powers of S and r (G&R, 1.332) gives expressions for $K_q^n(r, a)$ in terms of elliptic-type integrals,

$$\begin{aligned} K_{2q} = & \frac{(-1)^q}{8\pi} \sum_{u=0}^q (-1)^u \frac{[(2q+1)^2 - 1^2] \dots [(2q+1)^2 - (2u-1)^2]}{(2u)!} r^{2u-1} \\ & \times \sum_{v=0}^{2u} \binom{2u}{v} \left(-\frac{r+a}{r} \right)^{v-1} H_{n,1-v}(\lambda), \end{aligned} \quad (2.21)$$

$$\begin{aligned} K_{2q+1} = & (-1)^q \frac{(q+1)}{4\pi} \sum_{u=0}^q (-1)^u \frac{[(2q+2)^2 - 2^2] \dots [(2q+2)^2 - (2u)^2]}{(2u+1)!} r^{2u} \\ & \times \sum_{v=0}^{2u+1} \binom{2u+1}{v} \left(-\frac{r+a}{r} \right)^{v-1} H_{n,1-v}(\lambda), \end{aligned} \quad (2.22)$$

$$H_{n,m}(\lambda) = \int_{-\pi}^{\pi} \frac{\cos 2n\alpha}{(1 - \lambda^2 \cos^2 \alpha)^{m/2}} d\alpha, \quad \lambda^2 = \frac{4ra}{(r+a)^2}, \quad (2.23)$$

where the elliptic-type integral $H_{n,m}(\lambda)$ can be evaluated using published methods (Björkberg & Kristensson, 1987).

(c) Asymptotic behaviour of K_q^n for large q

To estimate K_{2q}^n for large q , we use the method of stationary phase (Bender & Orszag, 1978). This shows that

$$\int_a^b f(x) e^{i\lambda\phi(x)} dx \sim \left(\frac{2\pi}{\lambda|\phi''(x_0)|} \right)^{1/2} f(x_0) e^{i\lambda\phi(x_0) \pm i\pi/4} \quad \text{as } \lambda \rightarrow \infty, \quad (2.24)$$

where $\phi'(x_0) = 0$, $a < x_0 < b$ and we take the $+$ if $\phi''(x_0) > 0$ and the $-$ if $\phi''(x_0) < 0$. If there are several points of stationary phase, each one contributes. If $x_0 = a$ or b , the contribution is halved.

With (2.24) in mind, we write (2.19) as

$$K_{2q}^n = \frac{1}{\pi} (2q+1)(-1)^q \operatorname{Re}\{I(2q+1)\} \quad \text{with} \quad I(\lambda) = \int_0^\pi f(\psi) e^{i\lambda\beta(\psi)} d\psi, \quad (2.25)$$

where $f(\psi) = (\cos n\psi)/\{S(\psi) \cos \beta(\psi)\}$. We have $\sin \beta = S(\psi) - r$ so $\beta'(\psi) \cos \beta = S'(\psi) = (ra/S) \sin \psi$. Thus, the two endpoints, $\psi = 0$ and $\psi = \pi$ are points of stationary phase (where $\beta' = 0$). For the second derivatives, we have

$$\beta''(\psi) \cos \beta - (\beta')^2 \sin \beta = S''(\psi) = (ra/S^2)(S \cos \psi - S' \sin \psi).$$

Calculating, at $\psi = 0$, $S(0) = r - a$, $\sin \beta = -a$, $\cos \beta = \sqrt{1 - a^2}$, $S'' = ra/S(0)$ and $\beta''(0) > 0$. Similarly, at $\psi = \pi$, $S(\pi) = r + a$, $\sin \beta = a$, $\cos \beta = \sqrt{1 - a^2}$, $S''(\pi) = -ra/S(\pi)$ and $\beta''(\pi) < 0$. Hence,

$$\begin{aligned} I(\lambda) &\sim \frac{1}{2} \left(\frac{2\pi}{\lambda} \right)^{1/2} \left(\frac{f(0)}{\sqrt{|\beta''(0)|}} e^{i\lambda\beta(0) + i\pi/4} + \frac{f(\pi)}{\sqrt{|\beta''(\pi)|}} e^{i\lambda\beta(\pi) - i\pi/4} \right) \\ &= \left(\frac{\pi}{2\lambda ra} \right)^{1/2} \frac{1}{(1 - a^2)^{1/4}} \left(\frac{1}{\sqrt{r - a}} e^{-i\lambda\beta_1 + i\pi/4} + \frac{(-1)^n}{\sqrt{r + a}} e^{i\lambda\beta_1 - i\pi/4} \right) \end{aligned}$$

as $\lambda \rightarrow \infty$, where $\beta_1 = \arcsin a$ so that $\beta(0) = -\beta_1$ and $\beta(\pi) = \beta_1$. Thus, $I(\lambda)$ decays as $1/\sqrt{\lambda}$ and so, from (2.25), K_{2q}^n grows as \sqrt{q} :

$$K_{2q}^n \sim \sqrt{\frac{2q+1}{2\pi ra}} \frac{(-1)^q}{(1 - a^2)^{1/4}} \left(\frac{1}{\sqrt{r - a}} + \frac{(-1)^n}{\sqrt{r + a}} \right) \cos \{(2q+1)\beta_1 - \pi/4\}. \quad (2.26)$$

From (2.20), we have $K_{2q+1}^n(r, a) = 8(q+1)(-1)^q \operatorname{Im}\{I(2q+2)\}$, with $I(\lambda)$ defined by (2.25), so we obtain a similar estimate for K_{2q+1}^n as $q \rightarrow \infty$.

(d) Random disc source

The analysis given above can be extended to the case of a random source distributed over a disc. The starting point is an expression for the pressure radiated from a source distributed over a unit disc,

$$p(r, \theta, z, t) = \int_0^1 \int_{-\pi}^\pi \frac{q(a, \psi, t - R/c)}{4\pi R} dA, \quad (2.27)$$

where $dA = a d\psi da$, $R = \sqrt{r^2 + a^2 - 2ar \cos(\theta - \psi) + z^2}$ and c is the speed of sound. Then, the correlation between p measured at two points (r_1, θ_1, z_1) and

(r_2, θ_2, z_2) is

$$\begin{aligned} & \overline{p(r_1, \theta_1, z_1, t)p(r_2, \theta_2, z_2, t + \tau)} \\ &= \int_0^1 \int_{-\pi}^{\pi} \int_0^1 \int_{-\pi}^{\pi} \frac{\overline{q(a_1, \psi_1, t - R_1/c)q(a_2, \psi_2, t - R_2/c + \tau)}}{(4\pi)^2 R_1 R_2} dA_1 dA_2, \end{aligned} \quad (2.28)$$

where the correlation function is defined by

$$\overline{p_1(t)p_2(t + \tau)} = \lim_{T \rightarrow \infty} \frac{1}{2T} \int_{-T}^T p_1(t)p_2(t + \tau) dt. \quad (2.29)$$

Fourier transforming (2.28) with respect to τ gives the cross spectrum as

$$W_{12}(k) = \int_0^1 \int_{-\pi}^{\pi} \int_0^1 \int_{-\pi}^{\pi} \frac{e^{ik(R_2 - R_1)}}{(4\pi)^2 R_1 R_2} Q_{12}(k; a_1, \psi_1; a_2, \psi_2) dA_1 dA_2, \quad (2.30)$$

$$Q_{12}(k; a_1, \psi_1; a_2, \psi_2) = \int_{-\infty}^{\infty} \overline{q(a_1, \psi_1, t)q(a_2, \psi_2, t + \tau)} e^{i2\pi f\tau} d\tau, \quad (2.31)$$

where Q_{12} is the correlation between the source at two points (a_1, ψ_1) and (a_2, ψ_2) , and $k = 2\pi f/c$.

On the assumption of statistical axial symmetry, the source correlation can depend only on the angular separation between two points $\psi_2 - \psi_1$, so that Q_{12} and W_{12} can be expanded in Fourier series in azimuth,

$$Q_{12} = \sum_{n=-\infty}^{\infty} Q_{12}^{(n)}(a_1, a_2) e^{in(\psi_2 - \psi_1)}, \quad W_{12} = \sum_{n=-\infty}^{\infty} W_{12}^{(n)}(r_1, z_1; r_2, z_2) e^{in(\theta_2 - \theta_1)},$$

with

$$\begin{aligned} W_{12}^{(n)} &= \int_0^1 \int_{-\pi}^{\pi} \frac{e^{i(kR_2 + n\psi_2)}}{4\pi R_2} \left[\int_0^1 \int_{-\pi}^{\pi} \frac{e^{-i(kR_1 + n\psi_1)}}{4\pi R_1} Q_{12}^{(n)}(a_1, a_2) dA_1 \right] dA_2 \\ &= \sum_{q=0}^{\infty} \mathcal{L}_q(k, r_2, z_2) \int_0^1 \int_{-\pi}^{\pi} \frac{e^{-i(kR_1 + n\psi_1)}}{4\pi R_1} v_q^n(a_1, r_2) dA_1 \\ &= \sum_{q=0}^{\infty} \sum_{m=0}^{\infty} \mathcal{L}_q(k, r_2, z_2) \mathcal{L}_m^*(k, r_1, z_1) v_{qm}^n(r_1, r_2), \end{aligned} \quad (2.32)$$

where $R_j = \sqrt{r_j^2 + a_j^2 - 2a_j r_j \cos \psi_j + z_j^2}$ ($j = 1, 2$),

$$v_q^n(a_1, r_2) = \frac{1}{4(q+1)} \int_0^1 K_q^n(r_2, a_2) Q_{12}^{(n)}(a_1, a_2) a_2 da_2, \quad (2.33)$$

$$v_{qm}^n(r_1, r_2) = \frac{1}{4(m+1)} \int_0^1 K_m^n(r_1, a_1) v_q^n(a_1, r_2) a_1 da_1 \quad (2.34)$$

and an asterisk denotes complex conjugation.

(e) Low frequency behaviour

While the theory which has been presented so far is general and exact, it is worth examining the properties of the acoustic field at low frequency, $k \lesssim 2$, which have been examined before using an earlier version of the method (Carley, 2011). From (2.17) and (2.18), we have, exactly,

$$K_1^n(r, a) = 4\delta_{n0} - 4rK_0^n(r, a) \quad (2.35)$$

so that the resulting line source coefficients u_0^n and u_1^n are not linearly independent. This has been noted previously (Carley, 2011), using a different argument, and has an implication for the complexity of the low frequency acoustic fields. When $k \lesssim 2$, the field is dominated by the contributions of the first two line source modes. The fact that these modes will have the same coefficients, to within a scaling factor, means that the low frequency acoustic fields of disc sources are identical, whatever might be the details of the source proper. The implications of this finding for jet noise are considered in §4d.

3. Random cylindrical source

As a model problem for jet noise, and in particular of the modal decomposition methods and the near-to-far field correlation method used in studies of jet noise (Schlegel *et al.*, 2012; Laurendeau *et al.*, 2008), we consider a random source distributed over a cylindrical domain. The analysis for a random disc can be extended to the case of a cylindrical source of length $2L$ with axial coordinate $-L \leq z \leq L$, using the same non-dimensionalization as previously. The source cross-spectrum is $Q_{12}(k; a_1, \psi_1, b_1; a_2, \psi_2, b_2)$, with b_1 and b_2 source axial coordinates. Using the same symmetry arguments as previously, the cross-spectrum is decomposed,

$$Q_{12}(k; a_1, \psi_1, b_1; a_2, \psi_2, b_2) = \sum_{n=-\infty}^{\infty} Q_{12}^{(n)}(k; a_1, b_1; a_2, b_2) e^{in(\psi_2 - \psi_1)}, \quad (3.1)$$

and the azimuthal components of the cross-spectrum between two field points are given by

$$\begin{aligned}
 W_{12}^{(n)}(k; r_1, z_1; r_2, z_2) &= \int_{-L}^L \int_0^1 \int_{-\pi}^{\pi} \frac{e^{i(kR_2 + n\psi_2)}}{4\pi R_2} \\
 &\quad \times \left[\int_{-L}^L \int_0^1 \int_{-\pi}^{\pi} \frac{e^{-i(kR_1 + n\psi_1)}}{4\pi R_1} Q_{12}^{(n)}(k; a_1, b_1; a_2, b_2) dA_1 db_1 \right] dA_2 db_2, \\
 &= \sum_{q=0}^{\infty} \sum_{m=0}^{\infty} \int_{-L}^L \int_{-L}^L \mathcal{L}_q(k, r_2, z_2 - b_2) \mathcal{L}_m^*(k, r_1, z_1 - b_1) u_{qm}^n db_1 db_2, \quad (3.2)
 \end{aligned}$$

$$u_{qm}^n(r_1, b_1; r_2, b_2) = \int_0^1 \int_0^1 \frac{K_q^n(r_2, a_2) K_m^n(r_1, a_1)}{16(q+1)(t+1)} Q_{12}^{(n)} a_1 da_1 a_2 da_2 \quad (3.3)$$

4. Results

(a) Nature of acoustic field

A first set of conclusions can be drawn from the results for the radiation function $\mathcal{L}_q(k, r, z)$, in §2a. For large order q , the Bessel function $J_q(k)$ is exponentially small for $k < q$ so that the line source modes with order $q > k$ generate noise fields of exponentially small amplitude. Since $\mathcal{L}_q(k, r, z)$ has a maximum in the plane $z = 0$, (2.7) says that the whole field is of exponentially small amplitude. This gives an indication of how much of a given source distribution radiates into the acoustic field, as a function of wavenumber k and source order q , without recourse to near-field, far-field, or other approximations. Section 4b, giving sample calculations using full numerical evaluation of the appropriate integrals, compared to the line source method, shows that indeed the radiated field contains only terms due to line modes with $q \lesssim k$.

To demonstrate the character of the acoustic field of the line source modes, we plot \mathcal{L}_q for $k = 1.5$, figure 3, and $k = 6$, figure 4, for various values of q . The plots show logarithmically-spaced contours of the real and imaginary parts of the radiated field, similar to those of Chapman (1993), demonstrating the propagating wave character of the acoustic field, and the variation of amplitude with k .

Figure 3 shows the cut-off behaviour as q is increased above k . The $q = 0$ and $q = 1$ modes radiate efficiently into the whole field, as shown by the first two rows of contour plots. At $q = 2$, the field is already reduced in amplitude (note that the contour levels are the same in all plots) and the radiation pattern is becoming more directive, with less radiation into the near-axis region. At $q = 3$, the bottom row of figure 3, the field has almost disappeared, having only a small amplitude and being concentrated in a region near the source plane.

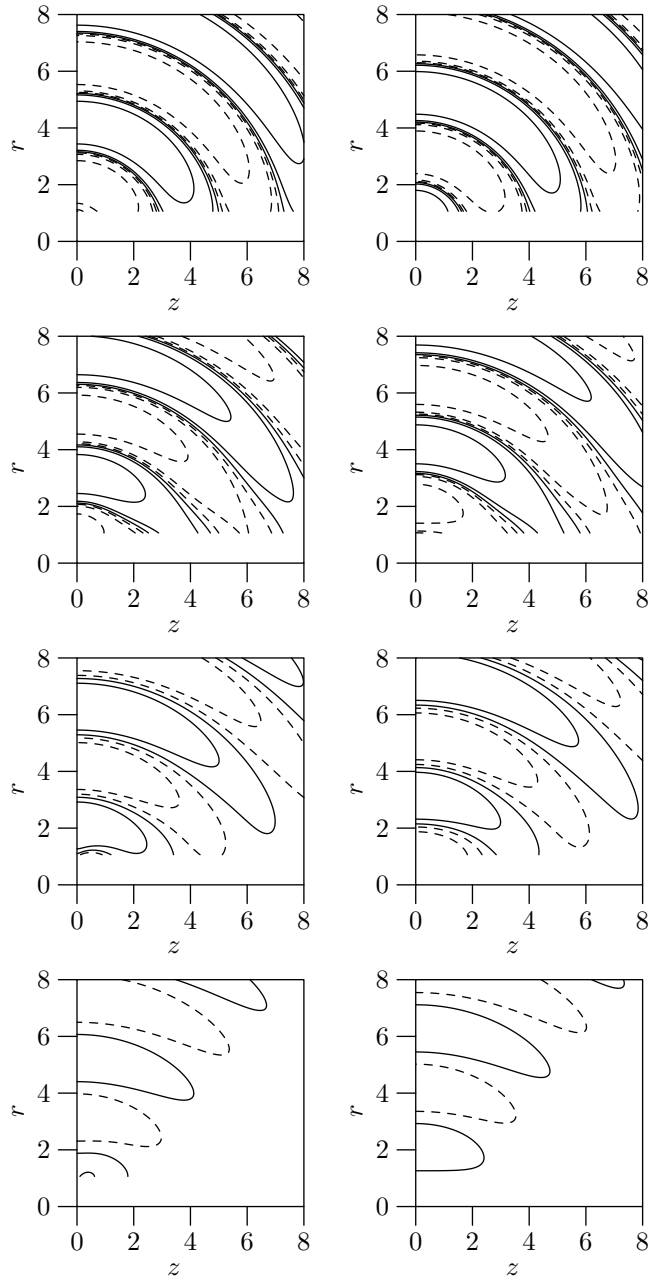


Figure 3. The function $\mathcal{L}_q(k, r, z)$ for $k = 1.5$, $q = 0, 1, 2, 3$, real part on left, imaginary part on right. Contour levels $\pm 2^{-5, -3, -1, 1}$, positive contours shown solid, negative shown dashed.

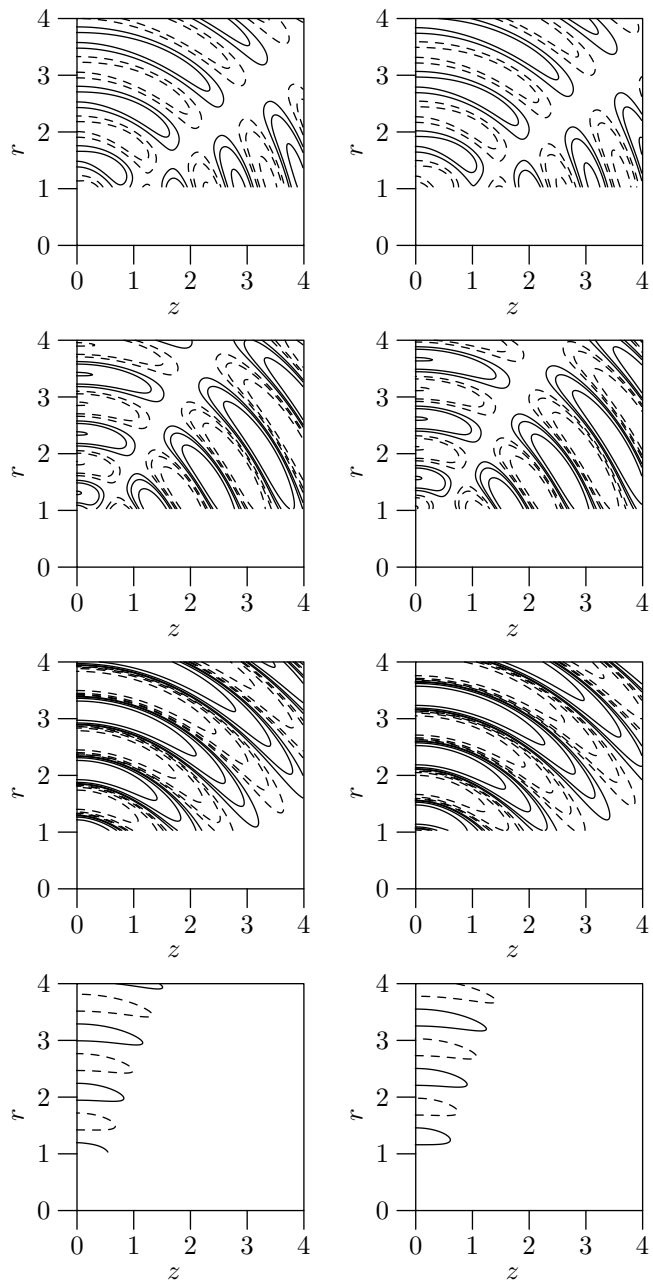


Figure 4. The function $\mathcal{L}_q(k, r, z)$ for $k = 6$, $q = 0, 1, 4, 8$, real part on left, imaginary part on right. Contour levels $\pm 2^{-3, -2, -1}$, positive contours shown solid, negative shown dashed.

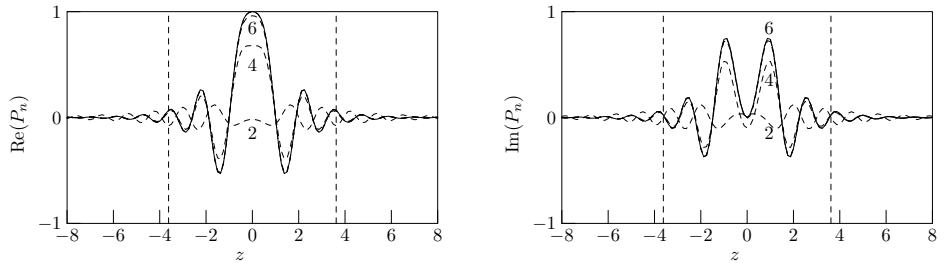


Figure 5. Convergence of line source method to full numerical integration for $n = 4$, $k = 6$, $r = 2$. Solid line: numerical integration; dashed lines: line source approach with 2, 4, 6 and 8 line source modes. Left: real part. Right: imaginary part. Vertical dashed lines indicate cut-off displacement for the $q = 5$ line mode. Results scaled on numerically evaluated value of P_n at $z = 0$.

Figure 4 shows similar behaviour, but with the higher wavenumber $k = 6$, the cut-off happens at a higher mode order, $q = 8$, and the lower order modes, especially $q = 0$ and $q = 1$, have a more complicated field pattern, with a pronounced null on a line through the origin. The $q = 4$ mode has a simpler directivity, but a greater amplitude, shown by the larger number of contours present: again, the same contour levels have been used in all plots.

(b) Numerical performance

As a check on the calculation method and on the convergence to the correct value of (2.1), figure 5 shows a sample evaluation of $P_n(k, r, z)$ using full numerical evaluation of the integral and the line source method with an increasing number of line source modes included, for $k = 6$ and $n = 4$. The radial source term $s_n(a) \equiv 1$. As predicted, the results for two and four modes do not capture the behaviour correctly, while six modes are sufficient to come very close to the correct result. When eight modes are included, the result is indistinguishable from full numerical evaluation.

For a random source, we assume a valid functional form for the source correlation, based on that given by Michalke (1983) for ring sources, with the addition of a radial correlation term,

$$Q_{12}(a_1, \psi_1; a_2, \psi_2) = q(a_1)q(a_2) \exp \left[-\frac{(a_1 - a_2)^2}{\beta^2} - \frac{1 - \cos(\psi_1 - \psi_2)}{\alpha^2} \right] \quad (4.1)$$

with α being an azimuthal length scale and β controlling the correlation in radius. Equation (4.1) can be interpreted as the product of the local source strengths $q(a_1)$ and $q(a_2)$ with a coherence function, given by the exponentials, which is symmetric in source position and has unit value when the source points coincide. For the calculations which follow, $q(a) \equiv 1$. The azimuthal components of Q_{12}

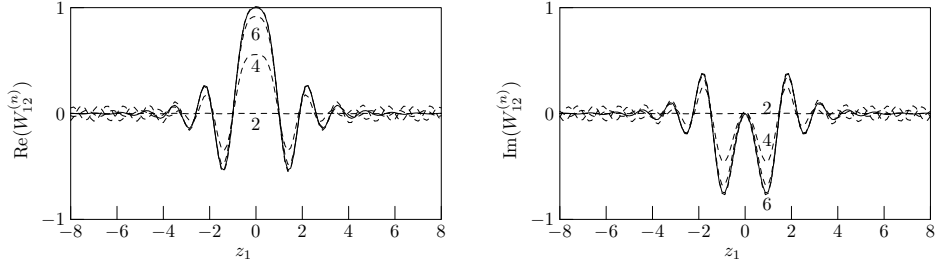


Figure 6. Convergence of line source method to full numerical integration for random disc $n = 4$, $k = 6$, $r_1 = 2$, $r_2 = 5/2$, $z_2 = 0$. Solid line: numerical integration; dashed lines: line source approach with 2, 4, 6 and 8 line source modes. Left plot, real part; right plot, imaginary part. Results scaled on numerically evaluated value of $W_{12}^{(n)}$ at $z_1 = 0$.

can be evaluated (Michalke, 1983) as

$$Q_{12}^{(n)}(a_1, a_2) = q(a_1)q(a_2) \exp \left[-\frac{(a_1 - a_2)^2}{\beta^2} \right] \exp \left[-\frac{1}{\alpha^2} \right] I_n(1/\alpha^2) \quad (4.2)$$

where I_n is a modified Bessel function.

Figure 6 shows similar results for a random disc source with the same parameters as in figure 5 and the correlation function parameters set to $\alpha = \beta = 1/2$. Again the effect of the number of line source modes included is demonstrated by the convergence to the full numerical evaluation, with the computed correlation given by a truncated series,

$$W_{12}^{(n)} = \sum_{q=0}^Q \sum_{m=0}^Q \mathcal{L}_q(k, r_2, z_2) \mathcal{L}_m^*(k, r_1, z_1) u_{qm}^n(r_1, r_2),$$

where $Q = 2, 4, 6, 8$. As before, when $Q \rightarrow k$, the line source results converge to the full numerical evaluation, with the higher order modes being ‘cut-off’ by the exponentially small amplitude of their radiated field.

Finally, we present a check on the evaluation of $W_{12}^{(n)}$ for a random cylindrical source. Here the correlation function has a Gaussian axial correlation term added,

$$Q_{12}(a_1, \psi_1, b_1; a_2, \psi_2, b_2) = e^{-\Omega} \exp \left[-\alpha^{-2} \{1 - \cos(\psi_1 - \psi_2)\} \right], \quad (4.3)$$

with $\Omega = [(b_1 - b_2)/\gamma]^2 + [(a_1 - a_2)/\beta]^2$ and

$$Q_{12}^{(n)}(a_1, b_1; a_2, b_2) = e^{-\Omega - \alpha^{-2}} I_n(1/\alpha^2). \quad (4.4)$$

Again, figure 7, the line source approach gives results indistinguishable from full numerical evaluation for $n \gtrsim k$. A last point to note is that the decomposition technique is very much faster than full numerical evaluation of the radiation

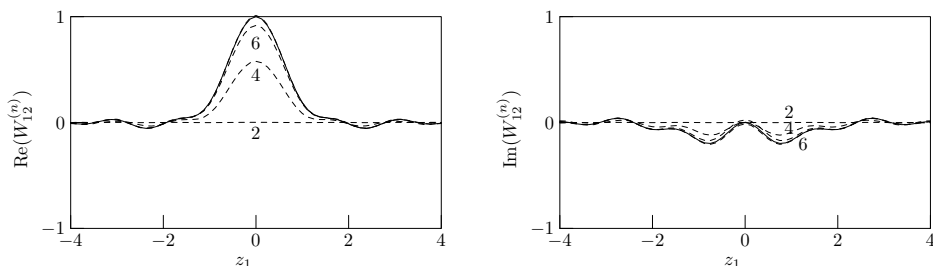


Figure 7. Convergence of line source method to full numerical integration for random cylinder $L = 1.0$, $n = 4$, $k = 6$, $r_1 = 2$, $r_2 = 5/2$, $z_2 = 0$. Solid line: numerical integration; dashed lines: line source approach with 2, 4, 6 and 8 line source modes. Left plot, real part; right plot, imaginary part. Results scaled on numerically evaluated value of $W_{12}^{(n)}$ at $z_1 = 0$.

integrals, especially if the field is to be evaluated at a large number of points, making it a practical noise prediction technique, as well as an analytical tool.

(c) Implications

The analysis presented so far has a number of implications for noise control and for source identification methods; jet noise is considered in §4d. The main point of the work presented is that it disconnects source from radiation effects, by condensing all of the information about the source into the coefficients u_q^n and all information about radiation into the function \mathcal{L}_q . It is then clear that the radiated acoustic field depends only on the non-dimensional wavenumber k , which fixes the number of line source modes which radiate, in effect fixing the number of source coefficients u_q^n which contribute to the final field.

The implication of this finding is that acoustic sources whose line source coefficients u_q^n differ only for $n \gtrsim k$ generate acoustic fields which cannot be distinguished from each other. In source identification problems, this means that the acoustic field, near or far, has only a finite number of degrees of freedom. Thus, any attempt to infer details of the source beyond this number of degrees of freedom is probably futile: the information about the source is not available in the acoustic field, even without considering the effects of background noise and other measurement errors. This may well explain the poor conditioning of many source identification methods, where the addition of large numbers of sensors has failed to improve the inversion technique.

The obverse of this observation is that if the acoustic field is to be controlled, only a finite number of degrees of freedom are required of an active controller, since only those parts of the source which actually contribute to the acoustic field need be controlled for. Similarly, if noise is to be reduced at source, the reduction effort should concentrate on reducing the contribution of those, lower order, modes which generate the perceptible acoustic field.

(d) *Jet noise*

An issue which has been of some interest for many years in studies of jet noise is the disparity between the complexity of the turbulent flow which gives rise to the noise field, and the relative simplicity of the field itself, exemplified by the finding that for a Mach 0.9 jet, 24 orthogonal modes were sufficient to capture 90% of the energy of the acoustic field, but 350 were required to resolve 50% of the flow energy (Jordan *et al.*, 2007). Various explanations have been put forward for this disparity, concentrating on the whole on mechanisms which affect radiation efficiency (Michel, 2007, 2009; Freund, 2001; Michalke, 1983), or discussing the distinction between a ‘source’ term, which radiates, and a ‘flow’ term, which does not (Sinayoko & Agarwal, 2012). The analysis presented in this paper gives an interpretation of the sources in terms of radiating and non-radiating terms, based purely on the properties of the acoustic source term, and the wavenumber of the radiation.

A first point to note is that the maximum noise level for a subsonic jet lies in a frequency range $k \lesssim 2$, with k based on the jet exhaust diameter. This means, as has been noted in experimental work, that the noise field is composed of azimuthal modes of order $n \lesssim 2$, as would be expected from the analysis this far. Thus, the observations made in §2e can be used to help explain certain features which have been noted in experimental studies of jet noise fields.

A recent paper (Schlegel *et al.*, 2012) generalizes the standard technique of Proper Orthogonal Decomposition (POD) to identify orthogonal modes of an aerodynamic field which contribute most to the observed, acoustic field. In a study of a Mach 0.9 jet, it was found (Schlegel *et al.*, 2012, figure 9) that 24 modes contribute 90% of the correlated noise. We tentatively propose, on the basis of the analysis given here, that such a small number of modes is a result of the radiation properties of the source, and that certain other features of the acoustic field can be explained using arguments based on the radiation properties outlined so far.

The standard theory of radiation from turbulent flows remains that of Lighthill (1952, 1954), although a number of theories modified for particular purposes or insights have been developed. The essential principle remains the same, however, in that the radiated noise, which here we view in terms of the cross-spectrum of the acoustic signal measured at two points in the field, is given, exactly, by an integral over the source region, where the source includes all mean and fluctuating flow effects (Lighthill, 1952, equation 15), subject to some differential operator,

$$W_{12}(k) = \sum_i \mathcal{D}_i \int_{b_1} \int_{b_2} \int_0^1 \int_{-\pi}^{\pi} \int_0^1 \int_{-\pi}^{\pi} \frac{e^{ik(R_2-R_1)}}{R_1 R_2} Q_{12}^{(i)} dA_1 dA_2 db_1 db_2, \quad (4.5)$$

where $Q_{12}^{(i)}$ is the cross-spectrum of the source at two points in the source volume, and index i runs over the different combinations of source term available, with \mathcal{D}_i being the spatial differential operator corresponding to a given

source combination. This approach, which lumps source and propagation effects together is supported by computational results (Bogey *et al.*, 2001). The source terms are given by the two-point, second and fourth order velocity correlations in the flow, and are not mutually uncorrelated. The analysis presented so far demonstrates that only a finite number of modes can radiate to the acoustic field, imposing a limit on the complexity of that field, without recourse to assumptions about the nature of the acoustic source or of the flow which gives rise to it.

Secondly, in another experimental study ‘the first POD mode is shown to give a near-perfect representation of the fluctuation energy radiation at low angles’, i.e., near the jet axis, ‘larger numbers of modes being necessary to completely reproduce the radiation characteristics at higher angles’, i.e., nearer the jet exhaust plane (Koenig *et al.*, 2010). These findings are readily explained by examination of figure 3, bearing in mind that the noise field is dominated by two line source modes, whose coefficients are not linearly independent, so that the field radiated by the source effectively has only one orthogonal mode per source term. In figure 3, the radiation pattern of the first four line source modes is shown and it is clear that the near-axis field only contains contributions from the first two modes, while \mathcal{L}_2 and \mathcal{L}_3 only appear nearer the source plane, and \mathcal{L}_3 then only very weakly. Again, we note that this is purely a result of the radiation properties of the source decomposition employed, and does not require that any assumptions be made about the nature of the source, of the aerodynamic processes which give rise to it, or whether the observer is in the near or far field, as in the earlier analysis of Michalke & Fuchs (1975).

5. Conclusions

We have presented an analysis which gives the radiated field of tonal and random disc sources without requiring near- or far-field approximations, splitting the problem into purely source-related terms and functions which affect only radiation. The nature and complexity of the radiated field are then fixed by the non-dimensional wavenumber of the source, showing, among other things, that low frequency sources generate indistinguishable fields. We conclude that many effects reported in the literature, such as the poor conditioning of source identification methods and the relative simplicity of jet noise fields, can be explained via our analysis, on the basis of the radiation characteristics of circular and cylindrical sources, without recourse to other arguments or approximations.

References

Bender, C. M. & Orszag, S. A. 1978 *Advanced mathematical methods for scientists and engineers*. McGraw-Hill.

- Björkberg, J. & Kristensson, G. 1987 Electromagnetic scattering by a perfectly conducting elliptic disk. *Can. J. Phys.*, **65**, 723–734.
- Bogey, C., Bailly, C. & Juvé, D. 2001 Noise computation using Lighthill's equation with inclusion of mean flow-acoustics interactions. In *7th AIAA/CEAS Aeroacoustics Conference*, AIAA 2001-2255.
- Carley, M. 2009 Inversion of spinning sound fields. *J. Acoust. Soc. Am.*, **125**, 690–697. (doi:10.1121/1.3050311)
- Carley, M. 2010 Analysis of the radiated information in spinning sound fields. *J. Acoust. Soc. Am.*, **128**, 1679–1684. (doi:10.1121/1.3478852)
- Carley, M. 2011 The radiating part of circular sources. *J. Acoust. Soc. Am.*, **129**, 633–641. (doi:10.1121/1.3531925)
- Castres, F. O. & Joseph, P. F. 2007a Experimental investigation of an inversion technique for the determination of broadband duct mode amplitudes by the use of near-field sensor arrays. *J. Acoust. Soc. Am.*, **122**, 848–859. (doi:10.1121/1.2747166)
- Castres, F. O. & Joseph, P. F. 2007b Mode detection in turbofan inlets from near field sensor arrays. *J. Acoust. Soc. Am.*, **121**, 796–807. (doi:10.1121/1.2427124)
- Chapman, C. J. 1993 The structure of rotating sound fields. *Proc. R. Soc. London. A.*, **440**, 257–271.
- Ffowcs Williams, J. E. 1984 Review lecture: Anti-sound. *Proc. R. Soc. London. A.*, **395**, 63–88.
- Freund, J. B. 2001 Noise sources in a low-Reynolds-number turbulent jet at Mach 0.9. *J. Fluid Mech.*, **438**, 277–305.
- Gérard, A., Berry, A., Masson, P. & Gervais, Y. 2007 Evaluation of tonal aeroacoustic sources in subsonic fans using inverse models. *AIAA J.*, **45**, 98–109. (doi:10.2514/1.21957)
- Goldstein, M. 1974 Unified approach to aerodynamic sound generation in the presence of solid boundaries. *J. Acoust. Soc. Am.*, **56**, 497–509.
- Gradshteyn, I. & Ryzhik, I. M. 1980 *Table of integrals, series, and products*. London: Academic, 5th edn.
- Holste, F. & Neise, W. 1997 Noise source identification in a propfan model by means of acoustical near field measurements. *J. Sound Vib.*, **203**, 641–665.
- Jordan, P., Schlegel, M., Stalnov, O., Noack, B. R. & Tinney, C. E. 2007 Identifying noisy and quiet modes in a jet. In *13th AIAA/CEAS Aeroacoustics Conference*. AIAA 2007-3602.

- Koenig, M., Cavalieri, A., Jordan, P., Delville, J., Gervais, Y., Papmoschou, D., Samimy, M. & Lele, S. 2010 Farfield filtering and source imaging for the study of jet noise. In *16th AIAA/CEAS Aeroacoustics conference*.
- Laurendeau, E., Jordan, P., Delville, J. & Bonnet, J.-P. 2008 Source-mechanism identification by nearfield-farfield pressure correlations in subsonic jets. *International Journal of Aeroacoustics*, **7**, 41–68.
- Lewy, S. 2008 Numerical inverse method predicting acoustic spinning modes radiated by a ducted fan from free-field test data. *J. Acoust. Soc. Am.*, **124**, 247–256. (doi:10.1121/1.2931952)
- Lighthill, M. J. 1952 On sound generated aerodynamically: I General theory. *Proc. R. Soc. London. A.*, **211**, 564–587.
- Lighthill, M. J. 1954 On sound generated aerodynamically II. Turbulence as a source of sound. *Proc. R. Soc. London. A.*, **222**, 1–32.
- Michalke, A. 1983 Some remarks on source coherence affecting jet noise. *J. Sound Vib.*, **87**, 1–17.
- Michalke, A. & Fuchs, H. V. 1975 On turbulence and noise of an axisymmetric shear flow. *J. Fluid Mech.*, **70**, 179–205.
- Michel, U. 2007 Influence of source interference on the directivity of jet mixing noise. In *13th AIAA/CEAS Aeroacoustics Conference*. AIAA-2007-3648.
- Michel, U. 2009 The role of source interference in jet noise. In *15th AIAA/CEAS Aeroacoustics Conference*. AIAA 2009-3377.
- Pierce, A. D. 1989 *Acoustics: An introduction to its physical principles and applications*. New York: Acoustical Society of America.
- Schlegel, M., Noack, B. R., Jordan, P., Dillmann, A., Gröschel, E., Schröder, W., Wei, M., Freund, J. B., Lehmann, O. *et al.* 2012 On least-order flow representations for aerodynamics and aeroacoustics. *J. Fluid Mech.*, **697**, 367–398. (doi:10.1017/jfm.2012.70)
- Sinayoko, S. & Agarwal, A. 2012 The silent base flow and the sound sources in a laminar jet. *J. Acoust. Soc. Am.*, **131**, 1959–1968. (doi:10.1121/1.3672804)